

Supporting Information

Opposing Effects of Side-Chain Flexibility and Hydrogen Bonding on the Thermal, Mechanical and Rheological Properties of Supramolecularly Cross-Linked Polyesters

Qianhui Liu[†], Chao Wang[‡], Yuanhao Guo[‡], Chao Peng[†], Amal Narayanan[†], Sukhmanjot Kaur[†], Ying Xu[†], R. A. Weiss^{‡,*}, Abraham Joy^{†,*}

[†] Department of Polymer Science, [‡] Department of Polymer Engineering, The University of Akron, Akron, Ohio 44325, USA

E-mail: abraham@uakron.edu; rweiss@uakron.edu

KEYWORDS: supramolecular crosslinking, hydrogen bonding, chain flexibility, functionalized polyesters

Contents

1. Experimental details of sample preparation for various characterizations
2. Variations in IR spectra with increases of temperature
3. Crazing as a toughening mechanism for P(1AP)
4. Rheological characterization of the three polyesters
5. Hygroscopic properties of samples
6. Static water contact angle measurement
7. NMR spectroscopies of pre-monomers and monomers
8. References

1. EXPERIMENTAL DETAILS OF SAMPLE PREPARATION FOR VARIOUS CHARACTERIZATIONS

Due to the hygroscopic properties of P(1AP) and P(2AP), various precautionary measures were taken to minimize moisture absorption in these polymers, before and during the tests.

Polymers were kept in vacuum oven for several days before the tests. For the DSC test, after the polymer was sealed in an aluminum pan, a hole was poked on the lid, and the sample was kept overnight in a vacuum oven. During the DSC test, temperature was increased to 140 °C and equilibrated for 5 min to facilitate removal of the residual moisture, and the T_g value was obtained from the second cycle of the run. The mechanical test was done when the air humidity was as low as 20-40%. Polymer thin films were made using a vacuum compression molding machine, and were cut into slices quickly. The tensile test was done right after sample preparation. In addition, specimens were kept in a small dessicator dried with desiccant-anhydrous drierite until tested. For the rheological test, specimens with diameter of 9 mm were prepared by vacuum compression molding machine and the test was done right away. Specimens were loaded and equilibrated at a temperature of 70 °C above T_g of each polymer, which was ~100 °C for P(1AP) and P(2AP) to allow the material to relax and remove any residual moisture. The rheological test was done at high temperature with a stream of air. Thermogravimetric analysis (TGA) was performed on the samples used in the mechanical and rheological tests right after those tests were done. No weight loss was observed on the TGA curve (the temperature was increased from 20 °C to 200 °C with

a heating rate of 10 °C /min). Theoretically, the water content of these specimens was zero.

2. VARIATIONS IN IR SPECTRA WITH INCREASE OF TEMPERATURE

IR spectra of the three polyesters

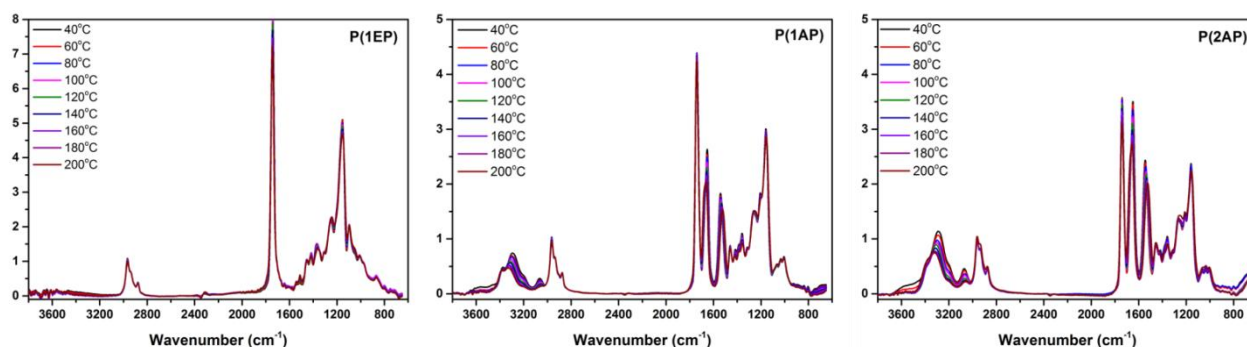


Figure S1. IR spectra of the three polymers normalized against C-H stretching peak.

Amide I & II modes and N-H stretching wavenumbers with increase of temperature of

P(1AP) and P(2AP)

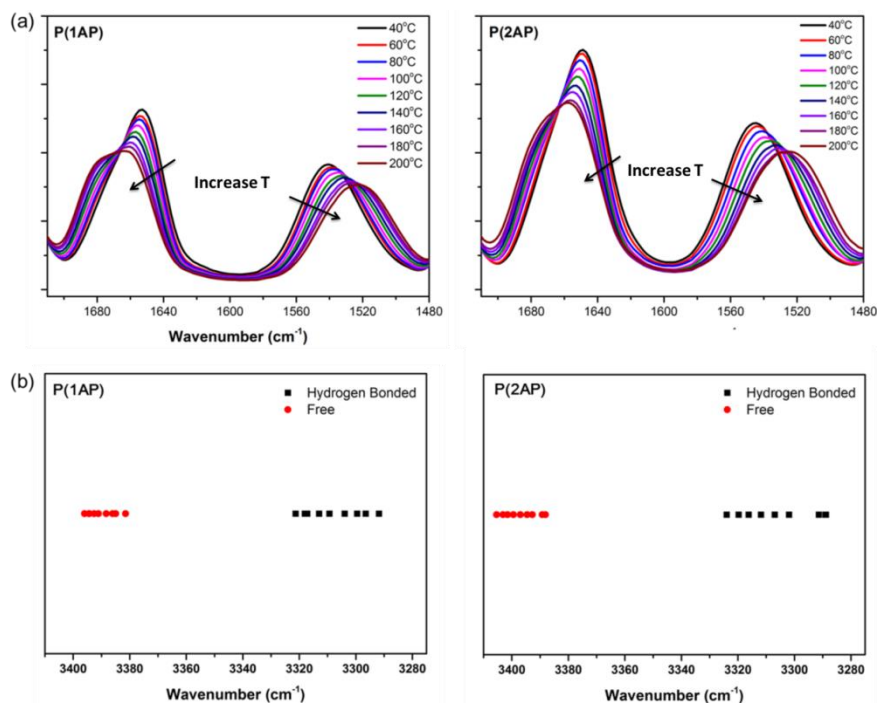


Figure S2. (a) Expanded spectra of amide I and amide II modes of P(1AP) and P(2AP)

at various temperatures. (b) H bonded and “free” N-H stretching peak shifting to higher wavenumber with increase of temperature.

3. CRAZING AS A TOUGHENING MECHANISM FOR P(1AP)

Morphology of fractured samples after tensile testing was characterized by SEM (JSM7401) and optical microscope. Samples with appropriate sizes were sputter coated with silver and the upper surfaces were observed with SEM. Optical microscope with different magnification times (50 x and 320 x) was used to observe samples.

During the stretching process it was observed that P(1AP) turned from transparent to white and this is observed in polymers which display crazing behavior. A craze is a precursor of crack and is bridged by many fibrils having diameters of a few tens of nanometers and length in orders of microns, and the fibrils are formed parallel to the stretching direction.^{1,2} As shown by optical microscopy, the voided regions in crazes leads to a change of refractive index and crazes in the sample appear white (**Figure S3(a)**). Due to the limit of resolution of our instrumentation, the SEM images did not show the extended fibrils (**Figure S3(b)**).

In this work, formation of crazing can also be reflected in the engineering stress-strain curve of P(1AP) (**Figure 3**). Stress at yield point is higher than that of the break point. Each polymer chain gains more and more strength during the stretching process, however, due to formation of crazing (the cavitation structure), only part of chains could bear the force (parts of the material already broke) and the total force decreases which results to a lower ultimate stress at break.

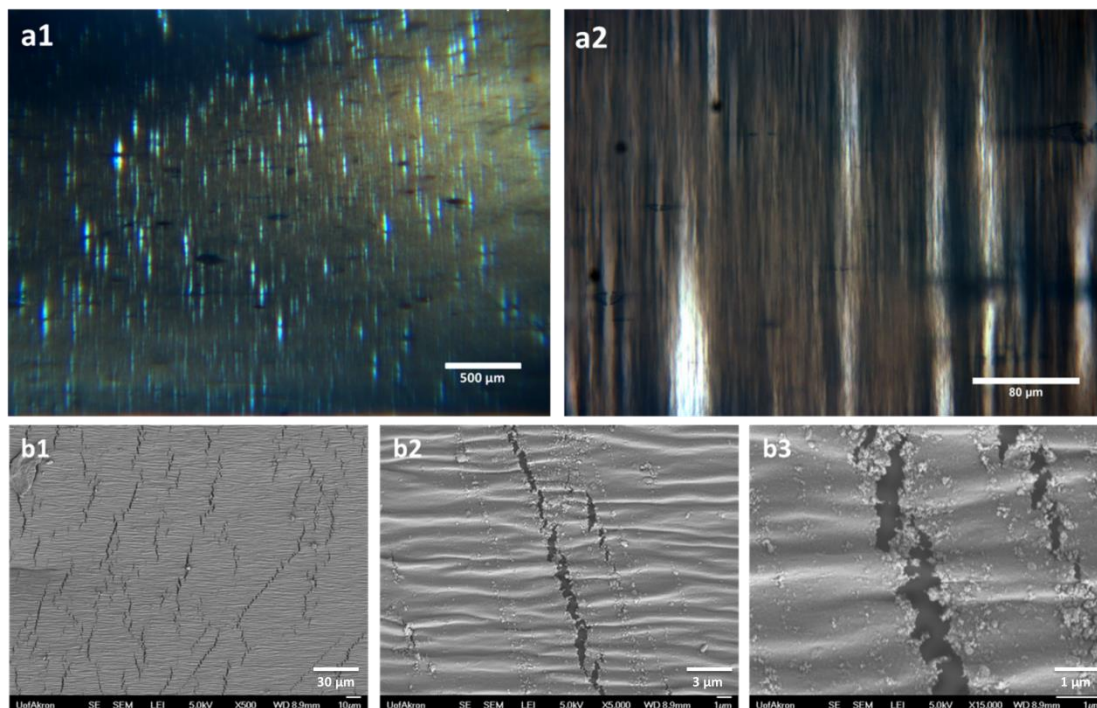


Figure S3. Observation of crazing using optical microscope with different magnification times (a1) 50 x, (a2) 320 x and SEM (b1, b2, b3)

4. RHEOLOGICAL CHARACTERIZATION OF THE THREE POLYESTERS

TTS curves and rheological properties of the three polymers at $T_r = 52\text{ }^{\circ}\text{C}$

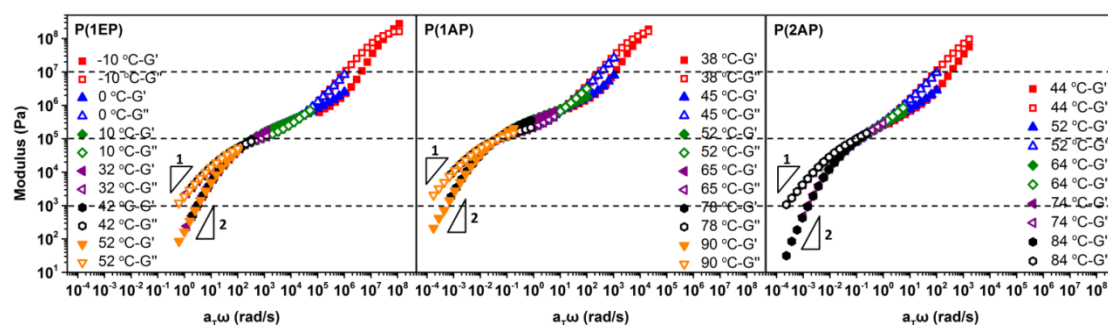


Figure S4. Comparison of the G' and G'' mastercurves for the three polymers compared at a common reference temperature of $52\text{ }^{\circ}\text{C}$.

Table S1. Rheological properties of three polymers according to TTS at $T_r = 52\text{ }^{\circ}\text{C}$.

	ω_t (rad/s)	ω_e (rad/s)	τ (s)	τ_e (s)	G_e (Pa)	η^*_{0} (Pa×s)
P(1EP)	1.95×10^2	2.56×10^4	3.22×10^{-2}	2.46×10^{-4}	4.80×10^5	1.86×10^3
P(1AP)	4.07×10^{-2}	1.49×10^1	1.54×10^2	4.21×10^{-1}	8.44×10^5	1.11×10^7
P(2AP)	2.90×10^{-1}	4.67×10^{-1}	2.16×10^1	1.34×10^1	2.02×10^5	4.57×10^6

Storage & loss modulus of the three polymers at $T_r = 52$ °C

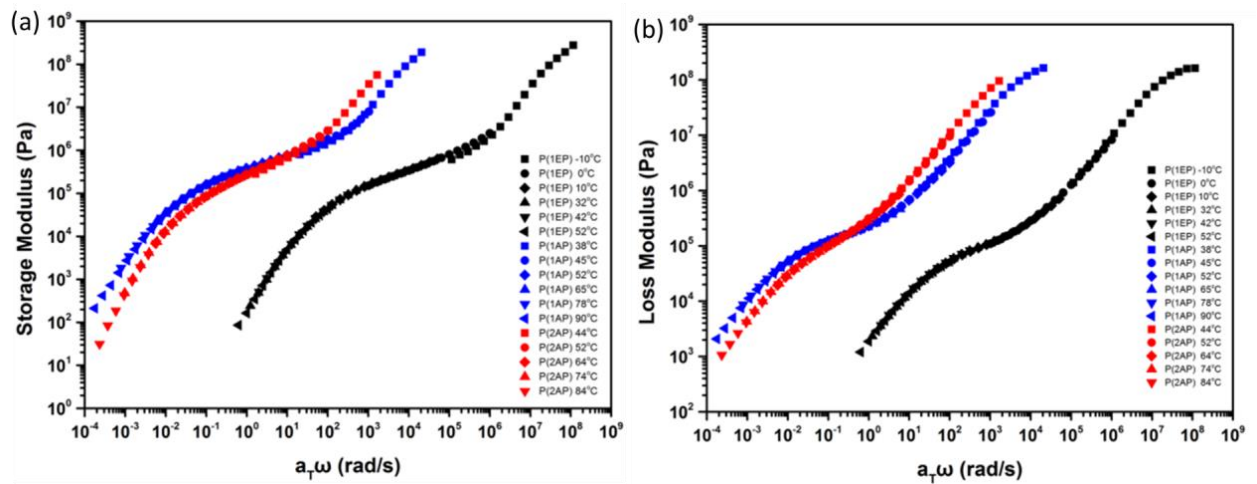


Figure S5. (a) Comparison of the G' for the three polymers at a reference temperature of $T_r = 52$ °C. (b) Comparison of the G'' for the three polymers at a reference temperature of $T_r = 52$ °C.

Complex viscosity of the three polymers at $T_r = 52$ °C

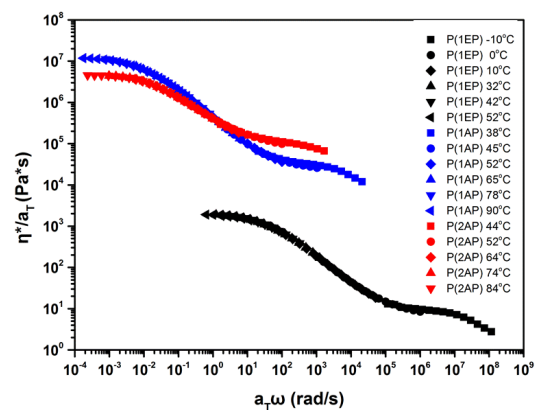


Figure S6. Comparison of the complex viscosity for the three polymers at a reference temperature of $T_r = 52$ °C.

Calculation of E_a for flow of the three polymers

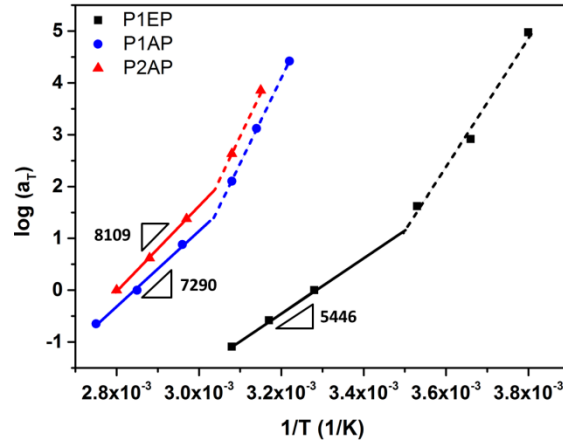


Figure S7. Relation between $\log(a_T)$ and $1/T$ for the three polymers

Curves of $\log(a_T)$ vs. $1/T$ of the three materials were plotted (a_T is the shift factor from TTS and T is Kelvin temperature). In **Figure S7**, there is an apparent turning point for each curve, which is the demarcation of WLF behavior and Arrhenius behavior. Linear fitting of the first few points (at high temperature where polymers obey Arrhenius equation) was done, and the slope of each curve was calculated. Based on Arrhenius equation, $\log a_T \propto E_a/RT$ (E_a is the activation energy for flow and R is gas constant), thus the activation energies for viscous flow were calculated as shown in **Table 4**.

Calculation of τ_l based on τ_2 and molecular weights

$$\tau \propto M_w^{3.4}. \quad M_w \text{ (P1AP): } 97.7 \text{ kDa; } M_w \text{ (P2AP): } 89.3 \text{ kDa; } \tau_{(P(1AP), 97.7 \text{ kDa})} = 1.21 \text{ s; } \tau_{(P(1AP), 97.7 \text{ kDa})} / \tau_{(P(1AP), 89.3 \text{ kDa})} = (M_w(P(1AP), 97.7 \text{ kDa}) / M_w(P(1AP), 89.3 \text{ kDa}))^{3.4}; \tau_{(P(1AP), 89.3 \text{ kDa})} = 0.891 \text{ s; } \tau_{(P(2AP), 89.3 \text{ kDa})} = 0.061 \text{ s.}$$

5. HYGROSCOPIC PROPERTIES OF SAMPLES

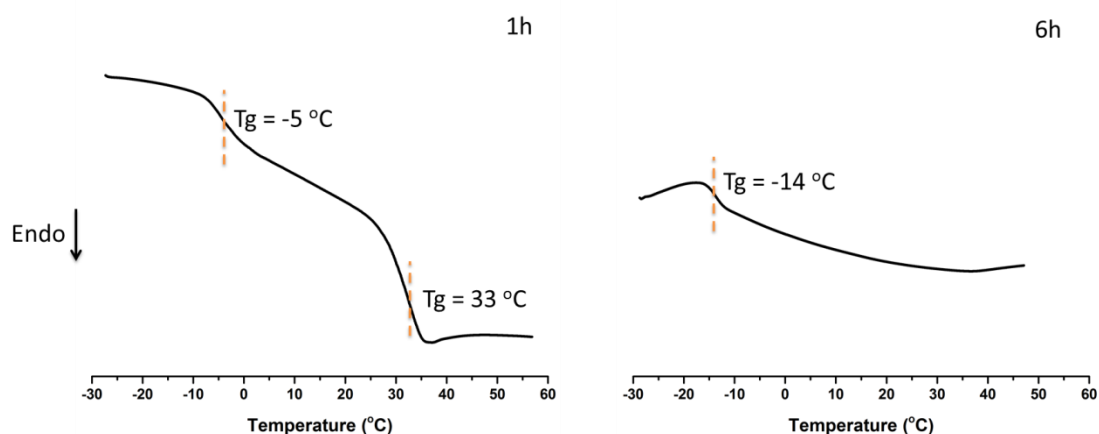


Figure S8. T_g s of P(2AP) after being exposed in humidifier for 1 h and 6 h. There are 2 T_g after P(2AP) was exposed to moisture for 1 h, and only one T_g after it was exposed for 6 h.

6. STATIC WATER CONTACT ANGLE MEASUREMENT

Polymer thin films were obtained by spin coating of filtered polymer solutions (20.0 mg polymer in 1 mL solvent, CHCl_3 for P(1EP), MeOH for P(1AP) and P(2AP)) on clean glass cover slips at room temperature by a spin coater. Cover slips were placed in vacuum oven at $60\text{ }^{\circ}\text{C}$ overnight to remove residual solvent and moisture, and to allow polymer chains to relax before the test. Water contact angle measurements were performed on a contact angle goniometer (Rame-Hart). One drop of ultrapure water ($10\text{ }\mu\text{L}$) was added onto the coated cover slip surface with a micro-syringe and the angle change of droplet was recorded every 10 sec by a camera with a total recording time of 2 mins. DROP image advanced software was used to measure contact angle by contour fitting algorithm.

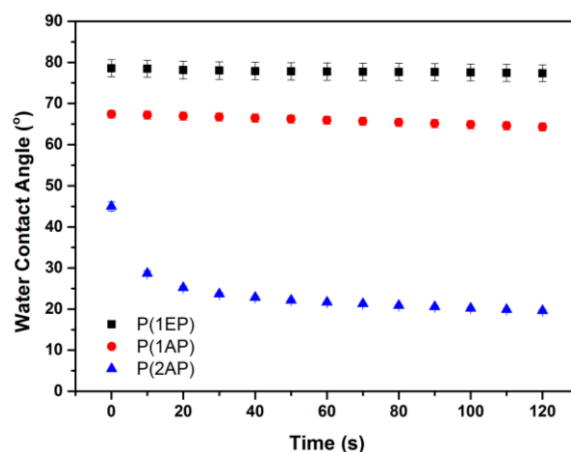
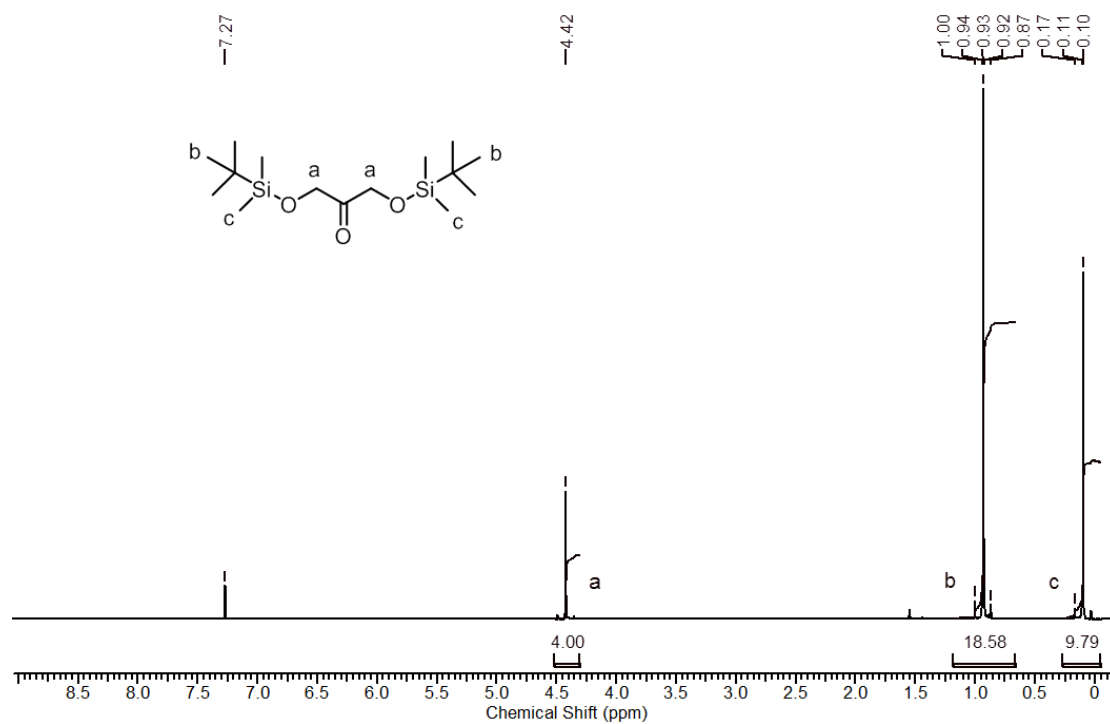


Figure S9. Record of water contact angle for the three polymers during 2 mins

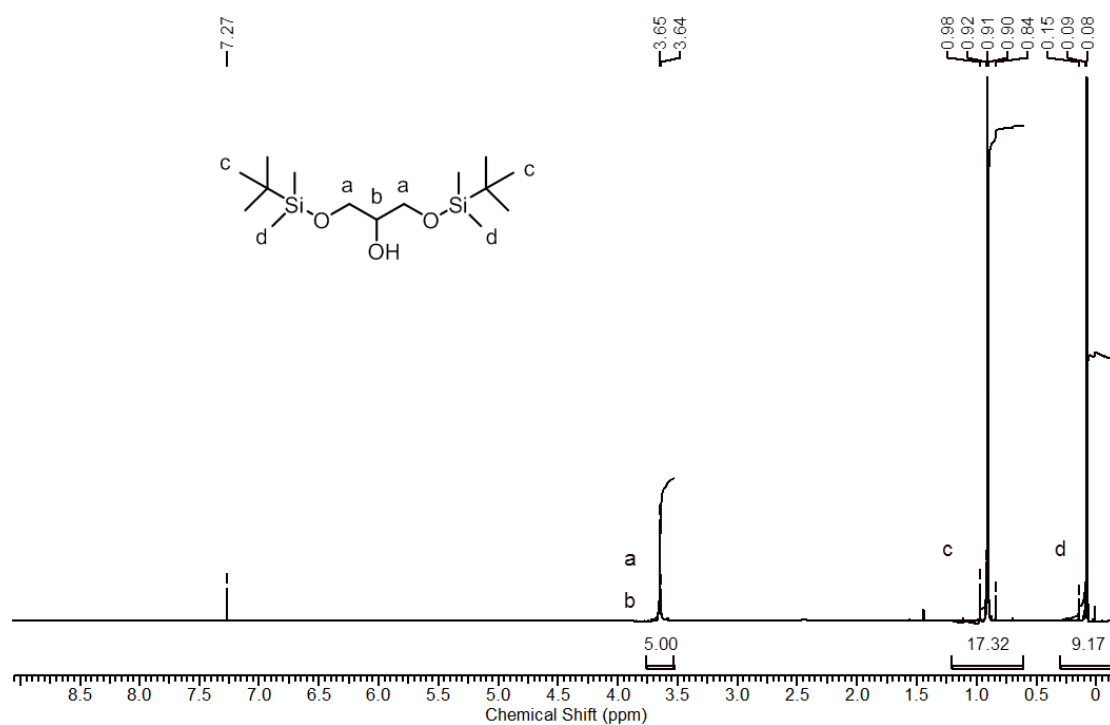
Different wetting phenomena with various polymer thin films were studied by water contact angle measurements. P(1EP) is the most hydrophobic material due to the highest contact angle value. The initial angle is 79° and it is independent of time during the test. P(1AP) has an initial contact angle of 67° and it decreases slightly over time. P(2AP) has the smallest initial contact angle which is 44°, and the angle value drops dramatically in first 10 seconds then levels off. The drastic drop of contact angle with P(2AP) results from molecular rearrangement of polymer chains on the surface, when the local environment changes from water vapor to liquid water.³ P(2AP) has a T_g of 34 °C, which is higher than room temperature, so the material is not supposed to rearrange in ambient environment. However, it was observed that rearrangement occurred. It is because the strength of hydrogen bonds decreases upon contact with water molecules, resulting in higher chain mobility. In this polymer system, it was concluded that the polymers hydrophilicity increases with increasing number of amide groups.

7. ¹H NMR SPECTROSCOPIES OF PRE-MONOMERS AND MONOMERS

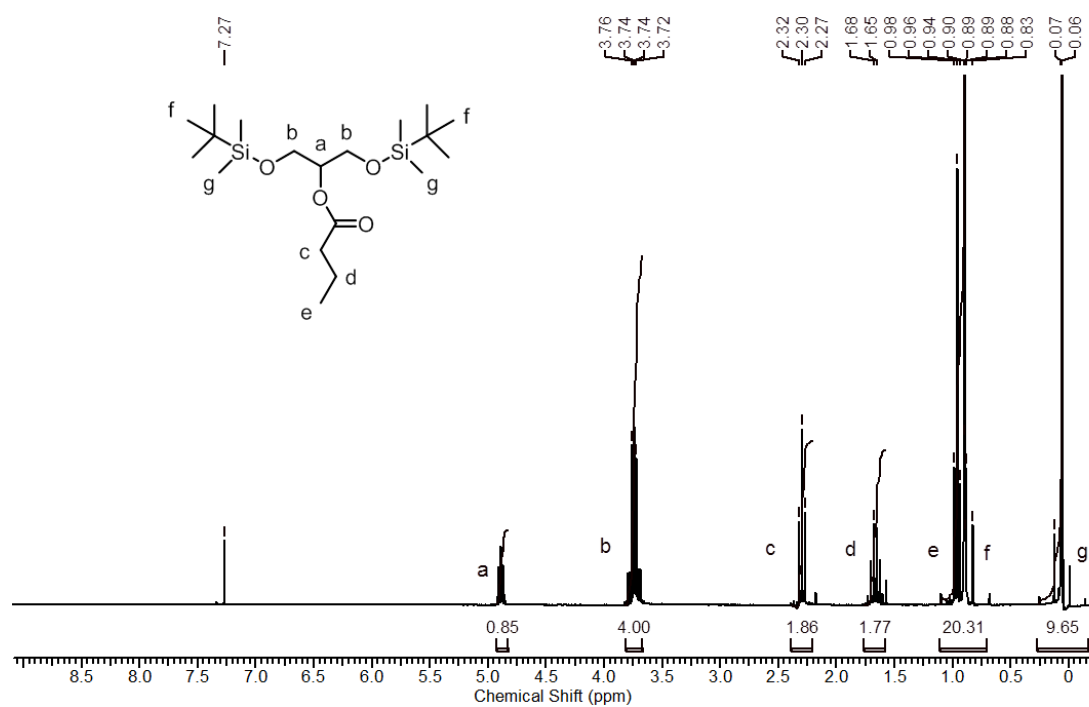
¹H NMR of compound in CDCl₃



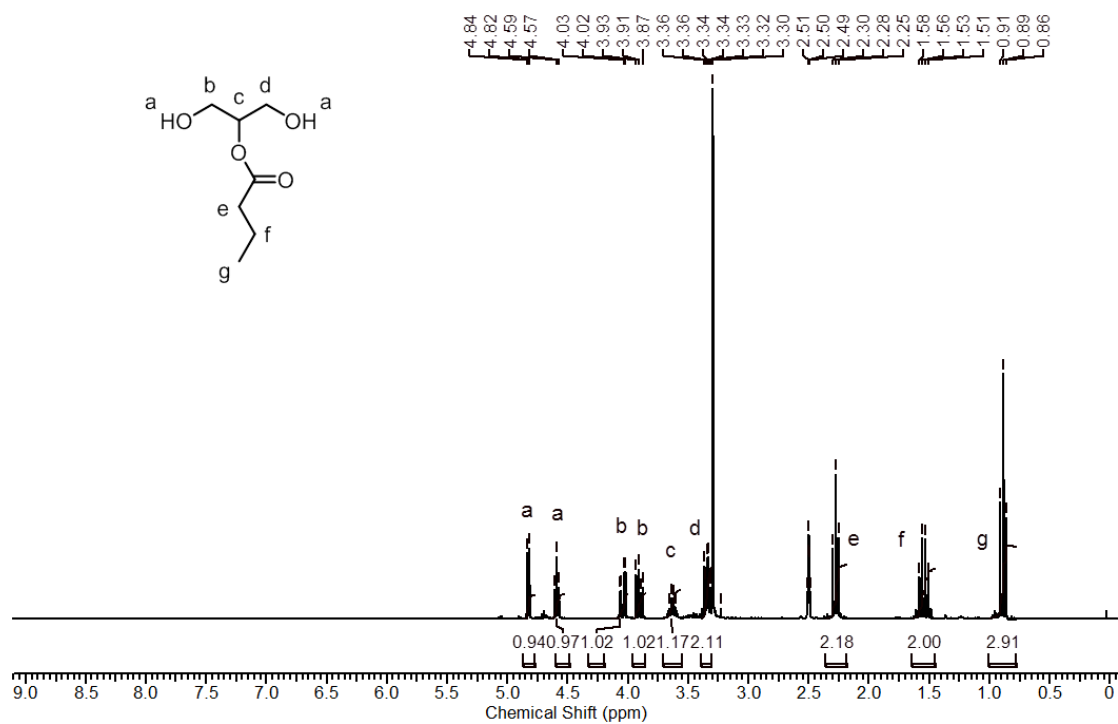
¹H NMR of compound in CDCl₃



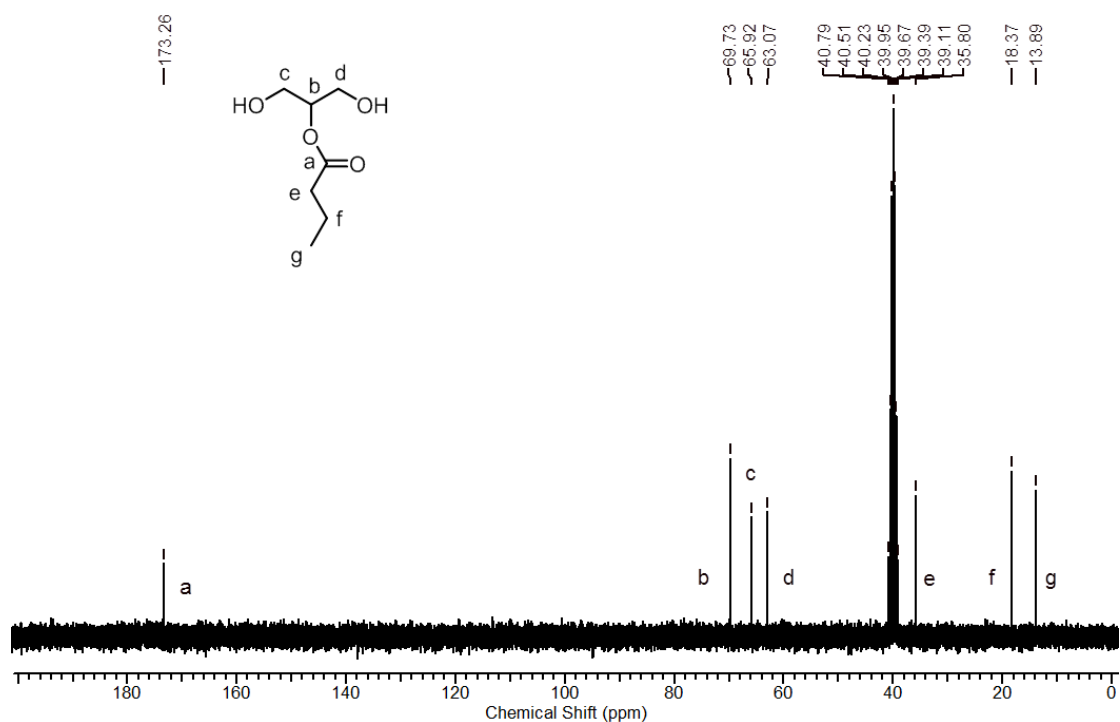
^1H NMR of compound in CDCl_3



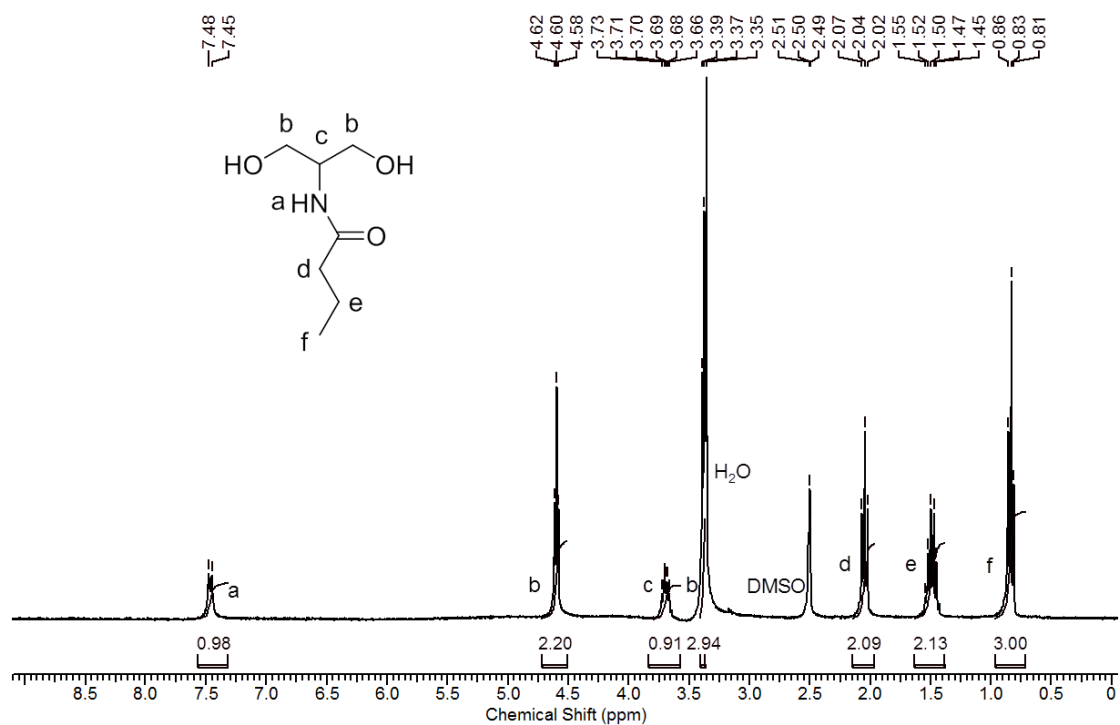
^1H NMR of compound in DMSO-d_6



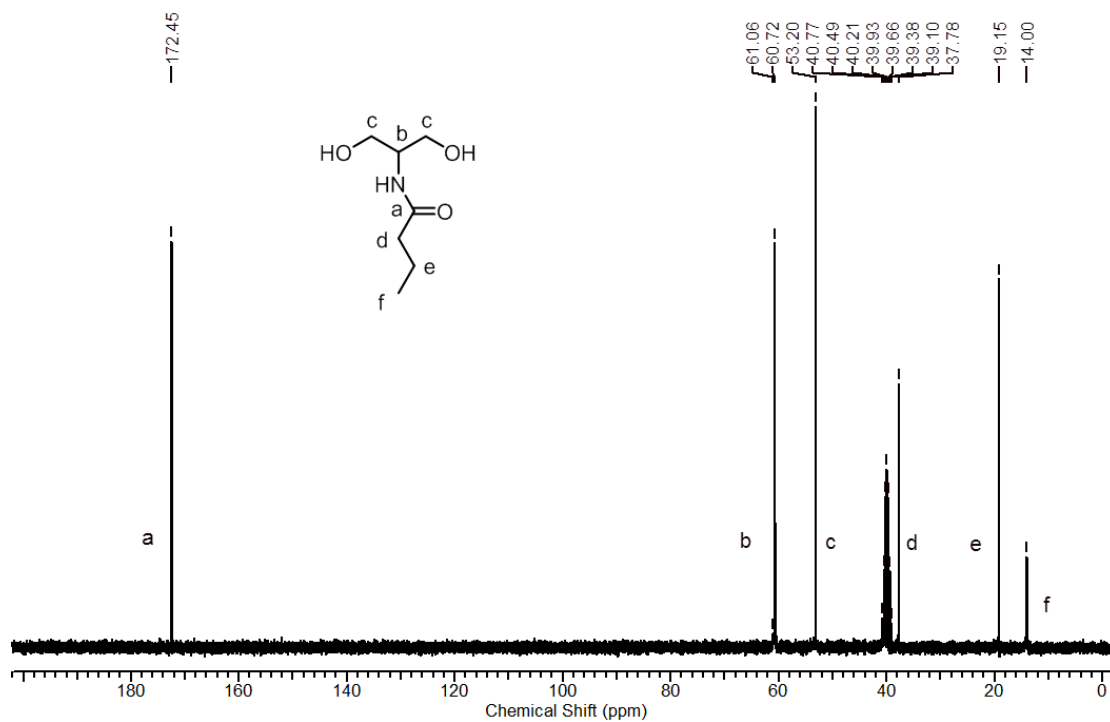
^{13}C NMR of compound in DMSO-d_6



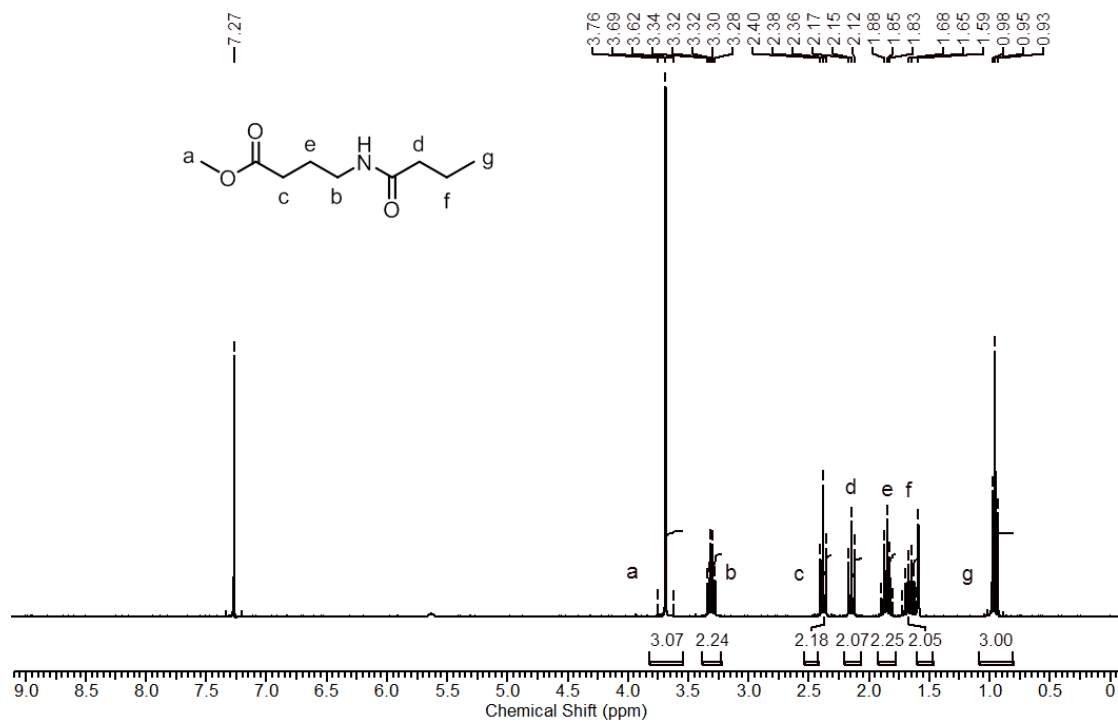
^1H NMR of compound in DMSO-d_6



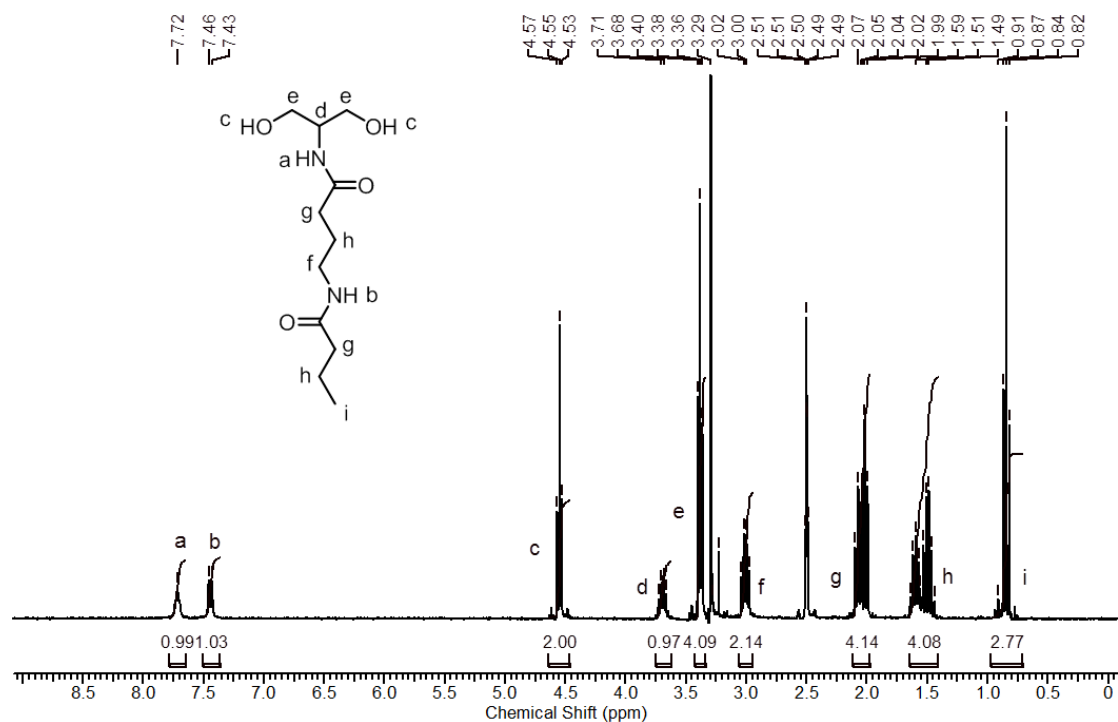
^{13}C NMR of compound in DMSO-d_6



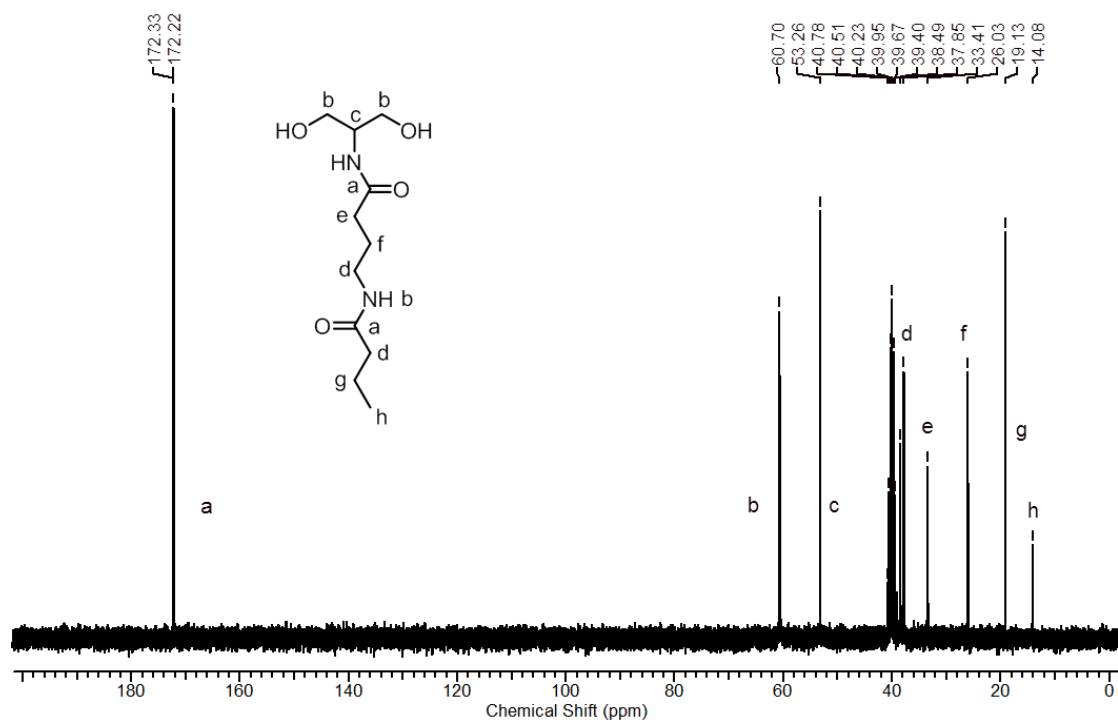
^1H NMR of compound in CDCl_3



^1H NMR of compound in DMSO-d_6



^{13}C NMR of compound in DMSO-d_6



8. REFERENCES

1. McLeish, T. C. B.; Plummer, C. J. G.; Donald, A. M., Crazing by disentanglement: non-diffusive reptation. *Polymer* **1989**, *30* (9), 1651-1655.
2. O'Connell, P. A.; McKenna, G. B., Yield and Crazing in Polymers. In *Encyclopedia of Polymer Science and Technology*, John Wiley & Sons, Inc.: 2002.
3. He, C.; Guiver, M. D.; Mighri, F.; Kaliaguine, S., Surface orientation of hydrophilic groups in sulfonated poly(ether ether ketone) membranes. *Journal of Colloid and Interface Science* **2013**, *409* (Supplement C), 193-203.